ELSEVIER

SCIENCE DIRECT®

PHYSICS LETTERS B

Physics Letters B 593 (2004) 75–81

www.elsevier.com/locate/physletb

# Photoproduction of $K^*$ for the study of $\Lambda(1405)$

T. Hyodo [a], A. Hosaka [a], M.J. Vicente Vacas [b], E. Oset [b]

[a] *Research Center for Nuclear Physics (RCNP), Ibaraki, Osaka 567-0047, Japan*

[b] *Departamento de Física Teórica and IFIC, Centro Mixto Universidad de Valencia—CSIC, Institutos de Investigación de Paterna, Aptd. 22085, 46071 Valencia, Spain*

Received 25 January 2004; received in revised form 20 March 2004; accepted 25 April 2004

Available online 1 June 2004

Editor: J.-P. Blaizot

**Abstract**

The photo-induced $K^*$ vector meson production is investigated for the study of the $\Lambda(1405)$ resonance. This reaction is particularly suited to the isolation of the second pole in the $\Lambda(1405)$ region which couples dominantly to the $\bar{K}N$ channel. We obtain the mass distribution of the $\Lambda(1405)$ which peaks at 1420 MeV, and differs from the nominal one. Combined with several other reactions, like the $\pi^- p \to K^0 \pi \Sigma$ which favours the first pole, this detailed study will reveal a novel structure of the $\Lambda(1405)$ state.



*PACS:* 13.60.-r; 13.88.+e; 14.20.Jn

*Keywords:* Chiral unitary approach; $\Lambda(1405)$

In recent years, we have been observing a remarkable development in hadron physics, especially in baryon resonances. Chiral models which implement strong $s$-wave meson–baryon interactions have been showing that some of the $1/2^-$ resonances, such as the $\Lambda(1405)$, are strongly dominated by quasi-bound states of coupled meson–baryon channels [1–4]. The case of the $\Lambda(1405)$ as a quasibound state is not a merit of the chiral Lagrangians since it was previously obtained in a unitary coupled channel approach in Refs. [5–7]. The use of chiral Lagrangians has allowed a systematic approach to face the meson–baryon interaction. In these pictures, the resonances generated may be regarded as another realization of 5-quark dominated states, although the lowest Fock space to generate the quantum numbers of $\Lambda$ starts from 3-quark states. The $s$-wave meson–baryon interaction at lowest order in the chiral Lagrangians is given by the Weinberg–Tomozawa term which contains an attractive interaction in the $\bar{K}N$ channel as well as its couplings to other meson–baryon channels. Therefore, confirmation of this picture is important in order to understand better the non-perturbative dynamics of QCD.

One interesting finding concerns the structure of the $\Lambda(1405)$ resonance; several groups have reported that there are two poles in the region of $\Lambda(1405)$

*E-mail address:* hyodo@rcnp.osaka-u.ac.jp (T. Hyodo).

0370-2693 © 2004 Elsevier B.V. Open access under CC BY license.
doi:10.1016/j.physletb.2004.04.065

in analyses based on the chiral unitary models [8–15]. The existence of two poles was first found in the context of the cloudy bag model [16], and recent studies of chiral dynamics reveal the detailed structure of these poles. For instance, in Ref. [17], they found two poles at $z_1 = 1390 - 66i$ MeV and $z_2 = 1426 - 16i$; the former at lower energy and with a wider width couples dominantly to $\pi\Sigma$ channels, while the latter at higher energy with a narrower width couples dominantly to $\bar{K}N$ channels. If this is the case, the form of the invariant mass distribution of $\pi\Sigma$, where the $\Lambda(1405)$ is seen, depends on the particular reaction used to generate the $\Lambda(1405)$ [17]. In fact, different shapes of mass distributions were observed in previous theoretical studies [18,19] and in Ref. [20] it was found that the $\pi^- p \to K^0\pi\Sigma$ reaction was particularly selective of the first $\Lambda$ pole. It is therefore desirable to study the nature of the $\Lambda(1405)$ focusing on whether such two poles really exist in the nominated resonance region.

In this Letter, we propose another, hopefully better, reaction induced by photons for the extraction of the second pole around the $\Lambda(1405)$ resonance: $\gamma p \to K^*\Lambda(1405) \to \pi K\pi\Sigma$. A great advantage of this reaction is the use of a linearly polarized photon beam and the observation of the angular distribution of $\pi K$ decaying from $K^*$, which is correlated with the linear polarization of the photon.

As we shall see below, if we produce a $\pi K$ system in a plane perpendicular to the photon polarization, the $t$-channel exchanged particle is dominated by the kaon; heavier strange mesons contributions should be suppressed due to their larger masses. Ignoring (hopefully small) background contributions from, for instance, unknown higher nucleon resonances also, it is sufficient to consider only the processes with kaon exchange, as shown in Fig. 1. The exchanged kaon rescatters in isospin $I = 0$ and 1 channels. Then the former couples strongly to $\Lambda(1405)$, especially to the higher pole, while the latter does it to $\Sigma(1385)$. We utilize the $s$-wave meson–baryon scattering amplitude calculated by the chiral unitary model [9,12]. The amplitude generates the $\Lambda(1405)$ resonance dynamically, while the $\Sigma(1385)$ is not generated because it is a $p$-wave resonance. In order to perform a realistic calculation, we introduce the $\Sigma(1385)$ field explicitly.

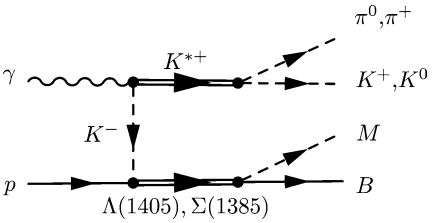


Fig. 1. Feynman diagram for the reaction. $M$ and $B$ denote the meson and baryon of ten coupled channels of $S = -1$ meson–baryon scattering. In this Letter we only take $\pi\Sigma$ and $\pi\Lambda$ channels into account.

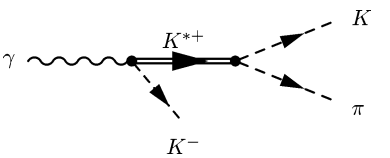


Fig. 2. Feynman diagram for $\gamma \to K^- K\pi$.

The scattering amplitude as described by the diagram of Fig. 1 can be divided into two parts

$$-it = (-it_{\gamma\to K^- K\pi})\frac{i}{p^2_{K^-} - m^2_{K^-}} \times (-it_{K^- p\to MB}). \tag{1}$$

The former part $(-it_{\gamma\to K^- K\pi})$, as shown in Fig. 2, is derived from the following effective Lagrangians [21,22]

$$\mathcal{L}_{K^*K\gamma} = g_{K^*K\gamma}\epsilon^{\mu\nu\alpha\beta}\partial_\mu A_\nu \times \left(\partial_\alpha K^{*-}_\beta K^+ + \partial_\alpha \bar{K}^{*0}_\beta K^0\right) + \text{h.c.}, \tag{2}$$

$$\mathcal{L}_{VPP} = -\frac{ig_{VPP}}{\sqrt{2}}\,\mathrm{Tr}\left(V^\mu[\partial_\mu P, P]\right), \tag{3}$$

where $K$, $A_\mu$, $V_\mu$ and $P$ are the kaon, photon, octet vector meson and octet pseudoscalar meson fields, respectively. The coupling constants are determined from the empirical partial decay width of $K^*$: $\Gamma_{K^{*\pm}\to K^\pm\gamma} = 0.05$ MeV and $\Gamma_{K^{*\pm}\to K\pi} = 51$ MeV. The resulting values are $|g_{\gamma K^{*\pm}K^\pm}| = 0.252$ [GeV$^{-1}$] and $g_{VPP} = -6.05$. The latter $g_{VPP}$ is the universal vector meson coupling constant. We note that the effective Lagrangian (2) is consistent with a vector meson dominance model [23]. Using the above interaction Lagrangians, the amplitude for $\gamma \to K^{*+}K^- \to$

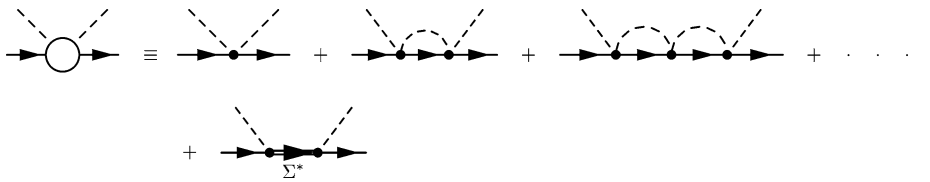


Fig. 3. Feynman diagram for $K^- p \to MB$.

$K^0\pi^+K^-$ is given by [1]

$$-it_{\gamma\to K^-K^0\pi^+} = \frac{i\sqrt{2}g_{VPP}\epsilon^{\mu\nu\alpha\beta}p_\mu(K^0)p_\nu(\pi^+)k_\alpha(\gamma)\epsilon_\beta(\gamma)}{P^2_{K^*}-M^2_{K^*}+iM_{K^*}\Gamma_{K^*}}, \tag{4}$$

where $p$ and $k$ are the momenta of the particle in parentheses, $\epsilon_\mu(\gamma)$ is the polarization vector of photon, and $\Gamma_{K^*}$ is the total decay width of $K^*$, for which we use the energy-dependent one for a virtual $K^*$, $\Gamma_{K^*} = Ap^3_{\rm CM}$, where $p_{\rm CM}$ is the two-body relative momenta of the final state, and $A = 2.05\times10^{-6}$ [MeV$^{-2}$] such that $\Gamma_{K^*}\sim 51$ MeV at the resonance position. Eq. (4) is instructive to show the correlations between the photon polarization and the $K^0$ and $\pi^+$ momenta. In order to maximize the contribution of the $t$-channel we select the $K^*$ in the direction of the photon. Then, it is easy to see that the amplitude is proportional to $\sin\phi$ where $\phi$ is the angle between the plane defined by the $K^0$ and $\pi^+$ momenta and the photon polarization (in the Coulomb gauge, $\epsilon^0 = 0$). Hence, the maximum strength of the amplitude occurs when this plane is perpendicular to the photon polarization.

In addition one needs not to worry about symmetrization in the case where there are two equal charge pions in the final state. In this case the interference term is zero and one can omit the symmetrization and the $1/2$ factor in the cross section.

The amplitude $(-it_{K^-p\to MB})$ consists of two parts, as shown in Fig. 3

$$-it_{K^-p\to MB}(M_I) = -it_{\rm ChU}(M_I) - it_{\Sigma^*}(M_I), \tag{5}$$

where $-it_{\rm ChU}$ is the meson–baryon scattering amplitude derived from the chiral unitary model, and $-it_{\Sigma^*}$ is the $\Sigma(1385)$ pole term. $M_I$ is the invariant mass for $K^-p$ system, which is determined by $M_I^2 = (p_\gamma + p_N - p_{K^*})^2$. In the chiral unitary model [9,12], the coupled channel amplitudes are obtained by

$$t_{\rm ChU}(M_I) = [1 - VG]^{-1}V, \tag{6}$$

where $G$ is the meson–baryon loop function and $V$ is the kernel interaction derived from the Weinberg–Tomozawa term of the chiral Lagrangian. This amplitude reproduces well the total cross sections for several channels. It also leads to dynamically generated resonances in good agreement with experiment. Since the $\Sigma(1385)$ is not generated in this resummation because it is a $p$-wave resonance, we introduce it explicitly with its coupling to channel $i$ ($\Sigma(1385)\to MB$) which is deduced from the $\pi N\Delta$ using $SU(6)$ symmetry in [24,25] and given by

$$-it_{\Sigma^* i} = c_i\frac{12}{5}\frac{g_A}{2f}(\boldsymbol{S}\cdot\boldsymbol{k}_i), \tag{7}$$

where $g_A = 1.26$, and we use the meson decay constant $f = 93\times1.123$ MeV [9]. This is a nonrelativistic form for the transition between spin $1/2$ and $3/2$ particles, where $\boldsymbol{S}$ is a spin transition operator [26] and the coefficients $c_i$ are given in Table 1. Note that these couplings reproduce well the observed branching ratio of $\Sigma(1385)$ decay into $\pi\Lambda$ and $\pi\Sigma$. Then we have the amplitude

$$-it_{\Sigma^*}(M_I) = -c_1c_i\left(\frac{12}{5}\frac{g_A}{2f}\right)^2(\boldsymbol{S}\cdot\boldsymbol{k}_1)(\boldsymbol{S}^\dagger\cdot\boldsymbol{k}_i) \times\frac{i}{M_I - M_{\Sigma^*}+i\Gamma_{\Sigma^*}/2}F_f(k_1), \tag{8}$$

where we have introduced a strong form factor $F_f(k_1)$ for the vertex $K^-p\Sigma^*$ in order to account for the finite size structure of the baryons. We adopt a monopole type $F_f(q) = (\Lambda^2 - m_K^2)/(\Lambda^2 - q^2)$ with $\Lambda = 1$ GeV. In the present reaction around the region of $\Lambda(1405)$, the effect of the form factor is not very large.

[1] For the final state $K^+\pi^0$, the amplitude is reduced by factor $1/\sqrt{2}$, and therefore, the resulting cross section becomes one half. In the rest of this Letter, we show the result for $K^0\pi^+$.

Table 1
$c_i$ coefficients

| Channel $i$ | $K^-p$ | $\bar{K}^0n$ | $\pi^0\Lambda$ | $\pi^0\Sigma^0$ | $\eta\Lambda$ | $\eta\Sigma^0$ | $\pi^+\Sigma^-$ | $\pi^-\Sigma^+$ | $K^+\Xi^-$ | $K^0\Xi^0$ |
|---|---|---|---|---|---|---|---|---|---|---|
| $c_i$ | $-\sqrt{\frac{1}{12}}$ | $\sqrt{\frac{1}{12}}$ | $\sqrt{\frac{1}{4}}$ | 0 | 0 | $-\sqrt{\frac{1}{4}}$ | $-\sqrt{\frac{1}{12}}$ | $\sqrt{\frac{1}{12}}$ | $\sqrt{\frac{1}{12}}$ | $-\sqrt{\frac{1}{12}}$ |

Table 2
Possible decay channels from baryons

| Intermediate baryon | Decay channels |
|---|---|
| $\Lambda(1405)$ $I=0$ | $\pi^\pm\Sigma^\mp$, $\pi^0\Sigma^0$ |
| $\Sigma(1385)$ $I=1$ | $\pi^\pm\Sigma^\mp$, $\pi^0\Lambda$ |

The cross section is then given by the squared amplitude of Eq. (1) integrated over the four-body phase space. After eliminating four momenta variables from the twelve momenta (of four particles), we can write a total cross section as a function of the incident energy $\sqrt{s}$:

$$\sigma\left(\sqrt{s}\right) = \frac{2MM_\Sigma}{s-M^2}\int\frac{d^3p_1}{(2\pi)^3}\frac{1}{2\omega_1}\int\frac{d^3p_2}{(2\pi)^3}\frac{1}{2\omega_2} \times\frac{1}{2}\int_{-1}^{1}d\cos\theta\frac{1}{4\pi}\frac{\tilde{P}_3}{M_I}\left|t(\cos\theta)\right|^2, \tag{9}$$

where $p_{1(2)}$ and $\omega_{1(2)}$ are the momenta and energy of the final $K(\pi)$ from $K^*$, and $\tilde{P}_3$ is the relative three momentum of $MB$ ($\sim\pi\Sigma$ or $\pi\Lambda$) in their center of mass frame. The angle $\theta$ denotes the relative angle of $MB$ in the CM frame of the total system. We have performed this integration by the Monte Carlo method. As we have mentioned before, the advantage of this reaction is that the identification of the $K^*$ production is cleanly done in experiments. Observation of the three pions in the process $K^{*+}\to\pi^+ + K^0\to\pi^+ + (\pi^+\pi^-)$ can be made with high efficiency and with all three momenta measured.

Before going to the numerical results, here we mention the $MB$ channels decaying from the intermediate baryonic state ($B^*\sim\Lambda(1405),\Sigma(1385)$). There are four possible $MB$ channels as shown in Table 2, two charged and two neutral channels. In the present case, since we have the $K^-p$ channel initially, the $I=2$ component of $\pi\Sigma$ channel is not allowed. Considering the Clebsh–Gordan coefficients [18], the charged channels ($\pi^\pm\Sigma^\mp$) are from the decay of both $\Lambda(1405)$ ($I=0$) and $\Sigma(1385)$ ($I=1$), while the neutral channels are from either one of the two; $\pi^0\Sigma^0$ is from $\Lambda(1405)$ and $\pi^0\Lambda$ is from $\Sigma(1385)$.

Now we present numerical results for total cross sections. Unless we observe angular distributions, there is not distinction between cross sections of polarized and unpolarized processes. Therefore, our predictions below are compared with the results of both polarized and unpolarized experiments directly. However, from the experimental point of view it is most practical to concentrate in the region where the $K^0\pi^+$ reaction plane is perpendicular to the photon polarization to maximize the weight of the $K^*$ production mechanism and reduce possible backgrounds. In Fig. 4, we show the total cross sections $\sigma(\gamma+p\to K^*+B^*\to\pi^+K^0+MB)$ as functions of $\sqrt{s}$ for different $MB$ channels. As seen in the figure, the present mechanism shows up strength at an energy slightly lower than the threshold of $K^*\Lambda(1405)\sim K^*\Sigma(1385)$ since the physical resonances have a finite width and hence a mass distribution. In the total cross section, the isospin one ($I=1$) $MB=\pi^0\Lambda$ channel is the largest in size, coming from $B^*=\Sigma(1385)$. This might disturb the contribution from $\Lambda(1405)$ of $I=0$, unless the separation of these two channels is done. However, it turns out that the observation of another charged $\pi$ from the intermediate baryon (either $\Lambda(1405)$ or $\Sigma(1385)$) helps.

In order to see this situation, we show in Fig. 5 the invariant mass distributions for different decay channels. In the figure the initial photon energy is chosen at $E_\gamma=2500$ MeV, the threshold energy for $K^*\Lambda(1405)$ production in the laboratory frame, which corresponds to $\sqrt{s}=2350$ MeV. Forgetting about the experimental feasibility, the would-be observable in the neutral channel is most helpful in order to distinguish the contributions from $\Lambda(1405)$ and $\Sigma(1385)$. As expected, the $\pi^0\Sigma^0$ distribution decaying from $\Lambda(1405)$ (solid line) has a peak around 1420 MeV which is the position of the higher pole. In contrast, the $\pi^0\Lambda$ distribution (dot-dashed line) has clearly a peak around 1385 MeV, with a larger value than the $\pi^0\Sigma^0$ distribution. In experiments, the charged states

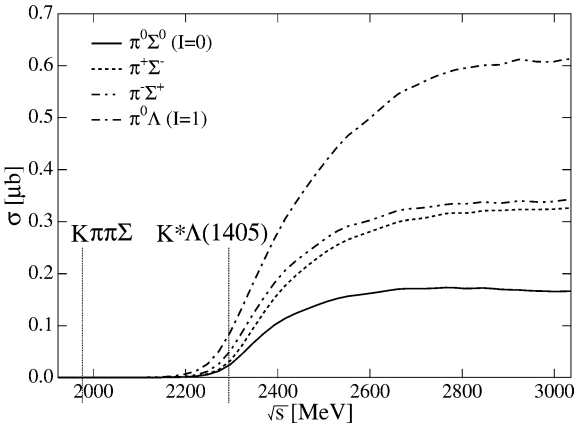


Fig. 4. Total cross sections of the process with the final states $\pi^0\Sigma^0$ (solid), $\pi^+\Sigma^-$ (dashed), $\pi^-\Sigma^+$ (dash-dot-dotted) and $\pi^0\Lambda$ (dash-dotted) in units of [μb]. Solid bars indicate the threshold energy of channels.

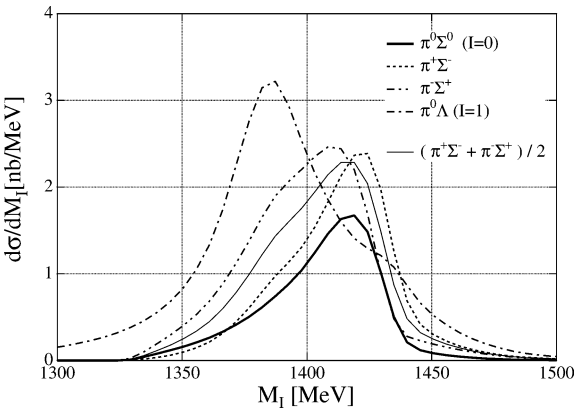


Fig. 5. Invariant mass distributions of $\pi^0\Sigma^0$ (thick solid), $\pi^+\Sigma^-$ (dashed), $\pi^-\Sigma^+$ (dash-dot-dotted), $\pi^0\Lambda$ (dash-dotted) and $(\pi^+\Sigma^- + \pi^+\Sigma^-)/2$ (thin solid) in units of [nb/MeV]. Initial photon energy in lab. frame is 2500 MeV ($\sqrt{s} \sim 2350$ MeV, threshold of $K^*\Lambda(1405)$).

may be observed, which contain both $\Lambda(1405)$ and $\Sigma(1385)$ contributions. Hence, we show the distribution of charged states by the dashed and dash-dot-dotted lines. The shapes of the three $\pi\Sigma$ distributions have a similar tendency as the Kaon photoproduction process [18], which has been confirmed in experiments [27]. Note also that the contributions from $\Sigma(1385)$ seem to be small for these channels.

It is worth showing the isospin decomposition of the distributions of charged states [18]

$$\frac{d\sigma(\pi^{\pm}\Sigma^{\mp})}{dM_I} \propto \frac{1}{3}\left|T^{(0)}\right|^2 + \frac{1}{2}\left|T^{(1)}\right|^2 \pm \frac{2}{\sqrt{6}}\,\mathrm{Re}\left(T^{(0)}T^{(1)*}\right),$$
$$\frac{d\sigma(\pi^0\Sigma^0)}{dM_I} \propto \frac{1}{3}\left|T^{(0)}\right|^2, \tag{10}$$

where $T^{(I)}$ is the amplitude with isospin $I$. The factor $1/2$ in front of $|T^{(1)}|^2$ and the ratio of the couplings $g^2_{\Sigma^*\pi^{\pm}\Sigma^{\mp}}/g^2_{\Sigma^*\pi^0\Lambda} = 1/3$ (see Table 1) explain why the $\Sigma(1385)$ does not affect the charged $\pi\Sigma$ channels very much, as compared with the $\pi\Lambda$ final state. The difference between $\pi^+\Sigma^-$ and $\pi^-\Sigma^+$ comes from the crossed term $\mathrm{Re}(T^{(0)}T^{(1)*})$, and when we sum up the two distributions this term vanishes. We also show the result for the sum of the charged $\pi\Sigma$ channels in Fig. 5 (thin solid line). The feature that the initial $K^-p$ couples dominantly to the second pole of the $\Lambda(1405)$ is well preserved in the total mass distribution, although the width of this distribution is slightly larger than that of the $I = 0$ resonance because it contains some contribution from the $\Sigma(1385)$. This is a nice feature and suggests that by observing the mass distributions of the charged state from the intermediate baryon, it would be possible to study the nature of the second pole of the $\Lambda(1405)$ resonance.

It is also interesting to see the $I = 1$ $s$-wave amplitude in this energy region, where the existence of another pole is discussed [8,17]. It was shown in Ref. [17] that in the $SU(3)$ decomposition of the meson baryon states the interaction was attractive in a singlet and two octets, hence it is natural to expect the existence of another $s$-wave $I = 1$ resonance in addition to the $\Sigma(1620)$ already reported in Ref. [9]. Indeed, a pole is found at $1410 - 40i$ MeV in the model of Ref. [8]. However, the properties of this $I = 1$ pole are very sensitive to the details of the model since in different models or approximations it appears in different Riemann sheets, but there is still some reflection on the amplitudes in all cases. Therefore, investigation of the $I = 1$ $s$-wave amplitude would bring further information of resonance properties.

We could have the $I = 1$ amplitude by combining the three $\pi\Sigma$ channels (see Eq. (10)). However, the $|T^{(1)}|^2$ term will contain contributions both from $s$ and

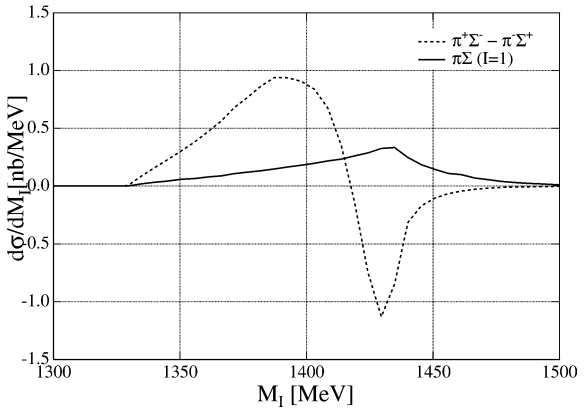


Fig. 6. Invariant mass distributions of $\pi^+\Sigma^- - \pi^-\Sigma^+$ (dashed), and $s$-wave, $\pi\Sigma(I=1)$ (solid), in units of [nb/MeV].

$p$-wave, although the contribution of the $p$-wave to the $\pi\Sigma$ channels is small. In order to extract the $I=1$ $s$-wave amplitude we separate the T-matrix into partial waves as

$$T^{(0)} = T_s^{(0)}, \qquad T^{(1)} = T_s^{(1)} + T_p^{(1)}. \tag{11}$$

Since we are looking at the cross sections where the angle variable among $MB$ is integrated, the product of $s$- and $p$-wave amplitude vanishes. Then, the difference of the distributions for the two charged states contains only the $T_s^{(1)}$ amplitude

$$\frac{d\sigma(\pi^+\Sigma^-)}{dM_I} - \frac{d\sigma(\pi^-\Sigma^+)}{dM_I} = \frac{4}{\sqrt{6}}\,\mathrm{Re}\big(T_s^{(0)}\big(T_s^{(1)}\big)^*\big). \tag{12}$$

We plot this magnitude in Fig. 6 with a dashed line. In principle, it is possible to extract $T_s^{(1)}$ from this quantity and the distribution of $s$-wave $I=0$ (for instance, from the $\pi^0\Sigma^0$), parametrizing conveniently the $T_s^{(0)}$ amplitude. Theoretically, in the present framework, we can calculate the pure $s$-wave $I=1$ by switching off the $\Sigma(1385)$ and making the combination of $\pi\Sigma$ amplitudes

$$\frac{d\sigma(\pi^+\Sigma^-)}{dM_I} + \frac{d\sigma(\pi^-\Sigma^+)}{dM_I} - 2\frac{d\sigma(\pi^0\Sigma^0)}{dM_I}. \tag{13}$$

The results are shown in Fig. 6 (solid line) and a small peak is seen as a reflection of the approximate resonant structure predicted in Refs. [8,17].

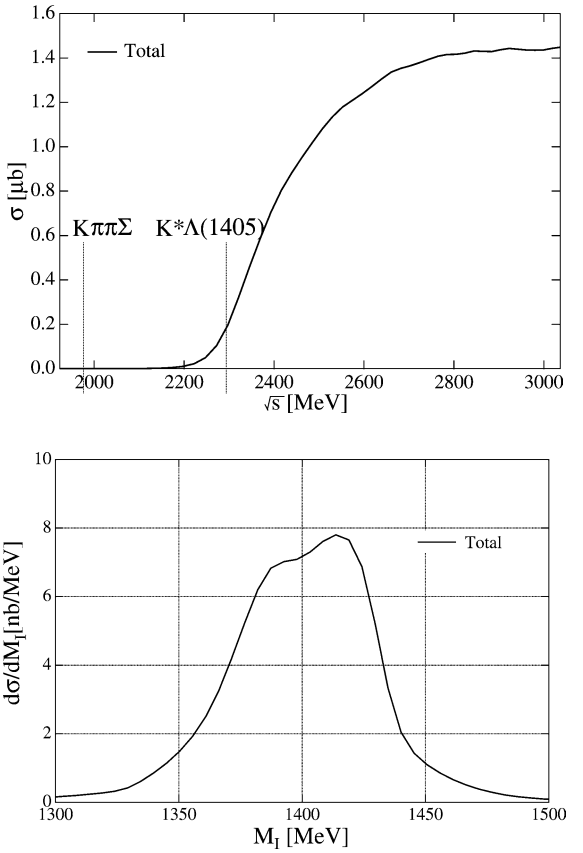


Fig. 7. Total cross section and invariant mass distribution for the sum of $\pi\Sigma$ and $\pi\Lambda$ channels.

Finally we show the results for the sum of all $\pi\Sigma$ and $\pi\Lambda$ channels in Fig. 7. This corresponds to the most feasible case in experiment in which the three pions decaying from $K^*$ are identified. In the total spectrum as a function of $M_I$ (right panel), we find a two-bump structure reflecting both the $\Lambda(1405)$ and the $\Sigma(1385)$. In the actual case, there would be a further contribution from the $\bar{K}N$ channel, raising at around 1430 MeV which we do not include in the calculation. This contribution starts where the mass distribution in Fig. 7 has already dropped down and therefore will not blur the shape of the distribution. This is the case in a related reaction studied in Ref. [18]. This figure is also illustrating because it reveals a large strength in the region of 1420 MeV, which makes this shape clearly distinct from the one observed experimentally in the $\pi^- p \to K^0\pi\Sigma$ reaction [28] with a neat peak around 1400 MeV.

Hence, this measurement is valuable by itself. Yet, to get the individual contributions one should measure the channels shown in Fig. 5. It is interesting to recall that in the chiral model of Ref. [20] it was shown that the $\pi^- p \to K^0 \pi \Sigma$ reaction favoured the lower mass $\Lambda$ pole.

In this Letter, we have proposed a reaction $\gamma p \to \pi^+ K^0 M B$ for the study of the second pole possibly existing in the $\Lambda(1405)$ region. This second resonance has been shown to couple more strongly to $\bar{K} N$ than to $\pi \Sigma$ in several chiral models, the present reaction is suitable for the isolation of this pole. Although the coupling to $\Sigma(1385)$ might contaminate the pure $\pi \Sigma$ mass distribution from the second $\Lambda(1405)$ pole, the resulting total mass distribution still maintains a peak structure pronounced around 1420 MeV with a relatively narrow width. The different shape of this mass distribution would be well differentiated from other experimental data for the $\Lambda(1405)$ excitation induced by other reactions, like the $\pi^- p \to K^0 \pi \Sigma$ [28] which favors the lowest energy pole at 1390 MeV as shown in Ref. [20]. A similar mass distribution to the present one was observed in the former study of $K^- p \to \gamma \pi \Sigma$ [19], where the photon is emitted from the initial state and hence the $\Lambda(1405)$ production is also induced by a $K^-$. Experimental evidence on the existence of such two $\Lambda^*$ states would provide more information on the nature of the current $\Lambda(1405)$ and thus new clues to understand non-perturbative dynamics of QCD.

## Acknowledgements

We would like to thank Prof. T. Nakano for suggesting this work to us. We also thank Dr. D. Jido for useful comments and discussions. This work is supported by the Japan–Europe (Spain) Research Cooperation Program of Japan Society for the Promotion of Science (JSPS) and Spanish Council for Scientific Research (CSIC), which enabled T.H. and A.H. to visit IFIC, Valencia and M.J.V.V. visit RCNP, Osaka. This work is also supported in part by DGICYT projects BFM2000-1326, and the EU network EURIDICE contract HPRN-CT-2002-00311.

## References

[1] N. Kaiser, P.B. Siegel, W. Weise, Nucl. Phys. A 594 (1995) 325.
[2] N. Kaiser, T. Waas, W. Weise, Nucl. Phys. A 612 (1997) 297.
[3] E. Oset, A. Ramos, Nucl. Phys. A 635 (1998) 99.
[4] M.F.M. Lutz, E.E. Kolomeitsev, Nucl. Phys. A 700 (2002) 193.
[5] R.H. Dalitz, S.F. Tuan, Ann. Phys. (N.Y.) 10 (1960) 307.
[6] R.H. Dalitz, T.C. Wong, G. Rajasekaran, Phys. Rev. 153 (1967) 1617.
[7] M. Jones, R.H. Dalitz, R.R. Horgan, Nucl. Phys. B 129 (1977) 45.
[8] J.A. Oller, U.G. Meissner, Phys. Lett. B 500 (2001) 263.
[9] E. Oset, A. Ramos, C. Bennhold, Phys. Lett. B 527 (2002) 99.
[10] D. Jido, A. Hosaka, J.C. Nacher, E. Oset, A. Ramos, Phys. Rev. C 66 (2002) 025203.
[11] C. Garcia-Recio, J. Nieves, E. Ruiz Arriola, M.J. Vicente Vacas, Phys. Rev. D 67 (2003) 076009.
[12] T. Hyodo, S.I. Nam, D. Jido, A. Hosaka, Phys. Rev. C 68 (2003) 018201.
[13] T. Hyodo, S.I. Nam, D. Jido, A. Hosaka, nucl-th/0305011, Prog. Theor. Phys., in press.
[14] C. Garcia-Recio, M.F.M. Lutz, J. Nieves, Phys. Lett. B 582 (2004) 49.
[15] S.I. Nam, H.-Ch. Kim, T. Hyodo, D. Jido, A. Hosaka, hep-ph/0309017.
[16] P.J. Fink, G. He, R.H. Landau, J.W. Schnick, Phys. Rev. C 41 (1990) 2720.
[17] D. Jido, J.A. Oller, E. Oset, A. Ramos, U.G. Meissner, Nucl. Phys. A 725 (2003) 181.
[18] J.C. Nacher, E. Oset, H. Toki, A. Ramos, Phys. Lett. B 455 (1999) 55.
[19] J.C. Nacher, E. Oset, H. Toki, A. Ramos, Phys. Lett. B 461 (1999) 299.
[20] T. Hyodo, A. Hosaka, E. Oset, A. Ramos, M.J. Vicente Vacas, Phys. Rev. C 68 (2003) 065203.
[21] Y. Oh, H. Kim, S.H. Lee, Phys. Rev. D 69 (2004) 014009.
[22] J.E. Palomar, E. Oset, Nucl. Phys. A 716 (2003) 169.
[23] A. Bramon, A. Grau, G. Pancheri, Phys. Lett. B 283 (1992) 416.
[24] E. Oset, A. Ramos, Nucl. Phys. A 679 (2001) 616.
[25] D. Jido, E. Oset, A. Ramos, Phys. Rev. C 66 (2002) 055203.
[26] G.E. Brown, W. Weise, Phys. Rep. 22 (1975) 279.
[27] LEPS Collaboration, J.K. Ahn, et al., Nucl. Phys. A 721 (2003) 715.
[28] D.W. Thomas, A. Engler, H.E. Fisk, R.W. Kraemer, Nucl. Phys. B 56 (1973) 15.